INVISCID THEORY OF WALL INTERFERENCE IN SLOTTED TEST SECTIONS*

Sune B. Berndt**
The Aeronautical Research Institute of Sweden (FFA)
S-161 11 Bromma 11, Sweden

Abstract

The classical theory of longitudinally slotted walls, which substitutes an approximate homogeneous wall boundary condition for the true mixed conditions, is extended in several respects. Based on recent experimental findings at the FFA, an inviscid flow model is adopted in which the outgoing slot flow penetrates into the plenum chamber as a thin jet, while the re-entering flow, admitting quiescent air from the plenum chamber into the test section, induces a longitudinal separation bubble at plenum pressure along the slot and adjacent parts of the test section wall. The three-dimensional analysis, based on the assumption that the slots are narrow, retains quadratic cross-flow terms in the pressure equation and allows the slots to be few in number and have non-uniform distribution and geometry. A family of homogeneous boundary conditions is obtained, each of successively higher accuracy. Application to the design of interference-free transonic test sections is discussed. Unsteady effects are also considered.

1. Introduction

It is a remarkable fact that theory plays a very minor roll in the design and use of slotted transonic test sections, in particular when one considers that the theory was already well developed at an early stage[1-3]. There might be several reasons for this but one of them seems to be that the flow models, mainly inviscid ones, had not been tested by careful experiments, while inconsistencies were alleged to appear in trying to apply the theoretical results to practical wind tunnel flows. Therefore, it seems, reliance was placed on empirical methods, determining the slot width so as to minimize choking effects around Mach one and accepting as free-stream conditions the upstream conditions in the empty test section as calibrated against the plenum pressure. It became a widespread belief that viscous effects of an unknown and complicated nature are present in the slot flow and that therefore an empirical approach is all there is available. In consequence the development of the theory came to a virtual standstill.

In a recent experimental investigation of slot flows[4] it has been found that under typical test conditions the slot flow is not necessarily dominated by viscosity and that therefore one can define an inviscid flow model which is reasonably close to reality. This model, which is not as simple as some of the early ones, will be set down in the next section. For a fuller discussion of the problems involved see Ref. 4 and references given therein.

Our present task is to base on this model a general inviscid theory for the wall interference caused by a slotted wall. In the classical theory of this kind[5-8], based on the slender-body approximation, a description is obtained of the combined effect of the mixed boundary conditions at the slots and slats in the form of a far simpler, homogeneous boundary condition, relating the average pressure difference across the wall to the average streamline curvature normal to the wall. The simplification is made possible by postulating a large number of similar slots uniformly distributed over the interfering wall.

In order to minimize any viscous effects, and possibly for other reasons, it is desirable to keep the number of slots small. Furthermore, if the slots are few in number their proper location might become important when minimizing the wall interference. Consequently there is a great need for freeing the classical theory from its inherent restrictions while keeping its simplicity. We shall achieve this by employing a modified method of approximation, based on the much less restrictive assumption that the slot width is small compared to the distance between slots. From the case of uniform slot distribution this is known to be a workable approach[9,10]. In the present more general context it leads to a straightforward application of the method of matched asymptotic expansions.

In our analysis we shall aim at a fair level of generality. This might for example facilitate later inclusion of corrections for viscous effects. The main concern will be with three-dimensional tests, the case of two-dimensional tests being already treated[4]. Also, we shall not exclude the case of unsteady flow, which is clearly quite important in connection with oscillatory testing[11]. However, in the present paper the applications of the theory will be restricted to a few very simple cases.

The theory turns out to produce not one but a whole family of possible homogeneous boundary conditions, each corresponding to a specific degree of resolution of the details of the wall flow as 'filtered' through the averaging procedure. The choice for any particular application will have to be based on considerations of accuracy. There is also some freedom in the method of applying the boundary conditions, depending on the kind of problem to be solved. If the slots are to be adjusted for zero interference by employing measured wall pressure distributions, a somewhat different type of boundary condition will be required from if the adjustment is to be based on a pre-computed interference-free flow field. We shall return to this point

* The research reported herein was sponsored jointly by the FFA and the US Air Force Office of Scientific Research (Grant No. AFOSR 72-2184).

** Consultant; also Professor of Gasdynamics, Royal Institute of Technology (KTH), S-100 44 Stockholm 70.

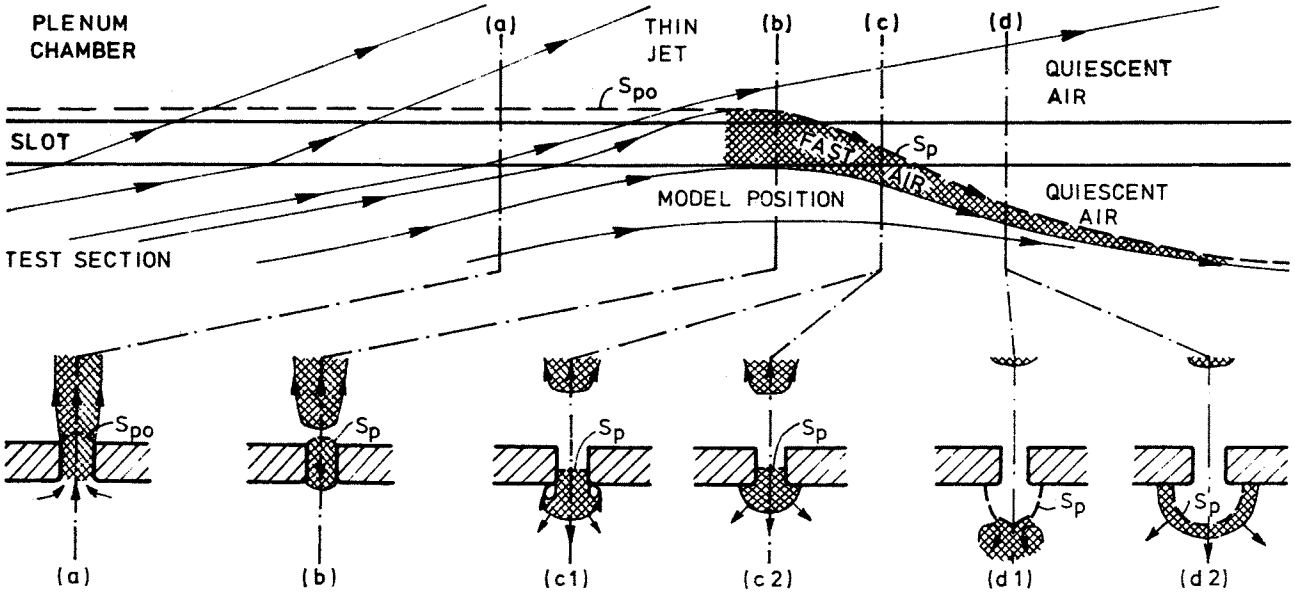

Fig. 1. Possible inviscid flow patterns (not to scale).
▒▒ = fast air from the slot.

in later sections as well as to the related questions of how to define and compute wall interference corrections and how to use test section calibrations.

2. An Inviscid Model for the Slot Flow

The slot flow model to be adopted is presented in Fig. 1. In the upstream part of the test section the flow is going outwards through the slot into the plenum chamber, where it forms a thin jet. The flow inside the slot is attached, as indicated in cross section (a), and separation occurs at the sharp slot edges on the plenum side. Above the model the slot flow turns back, leaving the jet to continue on its own into the interior of the plenum chamber. This 'splitting' of the fast air into two separate streams is shown beginning at section (b). At (c) the fast air in the slot, having entered farther upstream, is returning to the test section. At (d) the fast air has left the slot and behind it appears a 'bubble' of quiescent air at plenum pressure, the boundary of which is expanding into the test section flow. Typically, the bubble is narrow and extends along the slot. Presumably it collapses onto the slot farther downstream if the cross flow turns back again towards the wall. What happens if it is struck by a shock wave from the model is not known.

This is the picture of the slot flow arrived at in Ref. 4. The description leaves undecided whether the high speed air returning from the slot to the test section is a vorticity-carrying slug, as in (c1) and (d1), or whether it expands around the slot edges without separation, as in (c2) and (d2). The experimental evidence in Ref. 4, although not quite conclusive, points to the former alternative. It might well be that both types of flow may occur. In order to avoid complications at this stage we shall assume the second type of flow, but when developing the analysis we shall keep the alternative in mind as well as the possible need for viscous corrections.

In order to translate the slot flow model into a set of boundary conditions to be used with the flow equations further simplifications must be introduced. First of all there is no need to consider in detail the development of the jet inside the plenum chamber. From the point of view of the slot flow it should be sufficient to designate a surface S_{po} across the slot exit on which the plenum pressure may be taken to act. It must also be specified how the fast air in the slot is split off to return to the test section: making the obvious choice, we shall assume that the downstream end of S_{po} coincides with the upstream end of the free surface S_p, which is the boundary between the fast air and the quiescent plenum air (see Fig. 1). Thus S_{po} and S_p together form a surface on which we have plenum pressure. Obviously there is no need, nor any real possibility, to determine S_{po}, and hence S_p in its subsequent development, with any accuracy. We shall interpret this as a licence to make a choice which renders the analysis simple.

Having so far tacitly assumed that the flow is steady, we must also consider how the flow model can be generalized to become applicable to unsteady flows. Obviously, the free surface S_p must be allowed to move. The possibility that pressure waves propagate inside the plenum chamber must also be considered. Consequently, the pressure on $S_{po} + S_p$ cannot be taken to be known in advance. These are serious complications which can perhaps not be handled without making further simplifications, such as assuming the unsteadiness to be a small perturbation of a steady flow.

3. Assumptions and Basic Equations

The test section wall, before the slots are introduced, is taken to be a cylinder, S_w (Fig. 2). The longitudinal slots, numbered 1 to N, are connected to plenum chambers with quiescent air at prescribed pressures $p_p^{(i)}$ ($i = 1,2,..,N$). The x-axis, parallel to S_w, points

in the flow direction. The radius vector $\underset{\sim}{r}$ is orthogonal to the x-axis. The hydraulic radius of S_w is employed as the unit of length.

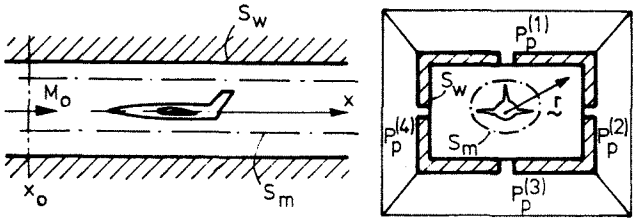

Fig. 2. Slotted test section.

The model and its wake are located within the cylinder S_m, parallel to S_w. The flow is taken to be inviscid between S_m and S_w, as well as in the slots and plenum chambers. The flow of fast air will be described by a small irrotational perturbation of a uniform reference flow parallel to the x-axis (at density ϱ_∞, pressure p_∞, velocity U and Mach number M), the perturbation to be considered as produced by the distribution of normal velocity set up by the model on S_m. This distribution is of course not known in advance. Our ignorance of the flow inside S_m is the reason for the wind tunnel test to begin with, but from the shape of the model one can often estimate it with sufficient accuracy for computing the wall interference. This we assume to be so and choose for the reference state the free-stream state at which the estimate is made.

Let $U \cdot \varphi(x,\underset{\sim}{r},t)$ be the perturbation velocity potential, normalized to be zero in the reference flow. To first order for transonic flow it satisfies the following differential equation between S_m and the outer boundary of the fast air:

$$\underline{\Delta}\,\varphi = \left[M^2 - 1 + M^2(\gamma+1)\varphi_x\right]\varphi_{xx} + \frac{2M^2}{U}\varphi_{xt} + \frac{M^2}{U^2}\varphi_{tt} . \qquad (1)$$

Here $\underline{\Delta}$ is the Laplacian in planes x = constant, while γ is the ratio of specific heats in the reference state. The inner boundary condition for φ is at a point P

$$\text{on} \quad S_m : \quad \varphi_n = F(P,t) \quad , \qquad (2)$$

where n denotes differentiation in the normal direction and F is the normal velocity distribution (which we have assumed known). The outer boundary condition on solid surfaces adjacent to fast air is similar:

$$\text{on} \quad S_w \quad \text{between slots:} \quad \varphi_n = 0 \ ,$$

$$\text{internally in slots:} \quad \varphi_n = H(P) \quad . \qquad (3)$$

H vanishes wherever the walls of the slots are parallel. (More generally, we could easily allow φ_n to be non-vanishing on S_w as well, thus accounting for small deviations from cylindrical geometry as well as for the displacement effect of wall boundary layers.)

The remaining outer boundary condition involves the pressure. In the present approximation the Bernoulli equation is

$$p - p_\infty = -\varrho_\infty U^2 \left(\frac{1}{U}\varphi_t + \varphi_x + \frac{1}{2}\,\mathrm{Grad}^2\varphi\right) , \qquad (4)$$

where Grad denotes the gradient operator in a plane x = constant. The quadratic cross-flow term is needed only in the slot regions, where the cross-flow velocity might be considerably larger than elsewhere. In the case of steady flow, the jet and free-surface boundary condition therefore takes the form

$$\text{on} \quad S_{po} + S_p \quad : \quad \varphi_x + \frac{1}{2}\,\mathrm{Grad}^2\varphi = -\,\delta^{(i)} \ ,$$

$$\delta^{(i)} \equiv \frac{p_p^{(i)} - p_\infty}{\varrho_\infty U^2} \quad (i = 1,\ldots,N) \ . \qquad (5)$$

The corresponding condition for unsteady flow will be discussed later.

In order to formulate an upstream boundary condition we shall assume that the slots all begin at $x = x_o$ and that their widths increase smoothly from zero. With a stretch of parallel walls between the contraction and the beginning of the slots — since F is likely to be small that far upstream — the flow at $x = x_o$ ought to be uniform (except for receding waves in the unsteady case). We shall in fact take this to be so and prescribe as an upstream boundary condition for steady flow that φ takes a constant value, φ_o say, on the plane $x = x_o$. At the same time we must adjust F to vanish at x_o. Note that the Mach number M_o of the entrance flow is a controllable test parameter which determines a particular value for φ_x. We shall not specify any downstream boundary condition, only assume that the slotted part of the test section is long enough for the conditions at the downstream end not to influence the flow at the model.

In the present approach the wall interference is obtained, obviously, by subtracting from φ on S_m the corresponding distribution obtained with unbounded flow outside S_m (using the same reference flow) in precisely the situation prescribed when estimating F. If we are to minimize the interference we must explore the influence on φ of the several test parameters at our disposal. The mixed form of the set of outer boundary conditions for φ constitutes a major difficulty when performing this task.

4. The Method of Approximation

In order to overcome this obstacle we shall introduce an approximation $\bar{\varphi}(x,\underset{\sim}{r},t)$ for φ, satisfying the same differential equation and the same inner boundary condition, but a new outer boundary condition. This boundary condition ought to be as simple as possible from the point of view of computing $\bar{\varphi}$, consistent with the requirement that $\bar{\varphi}$ must be closely equal to φ on S_m (where the interference is to be computed). Thus, the new boundary condition shall be required to be homogeneous and local in the sense that it is a regular functional relationship between $\bar{\varphi}$ and its normal derivative over the entire boundary S_w, while values of $\bar{\varphi}$ or $\bar{\varphi}_n$ inside S_w, e.g. on S_m, must not be explicitly present. Clearly the boundary conditions for φ are not homogeneous in this sense, although they are local.

The potentials $\bar{\varphi}$ and φ are expected to be nearly equal almost everywhere, in particular in the neighbourhood of S_m, and to be essentially different only where slots are located. There the cross-flow derivatives, but not the potentials themselves or their derivatives with respect to x or t, are expected to be much different. Noting that the differential equation (1) contains cross-flow derivatives only in the left-hand member, we arrive at our basic method of approximation: we neglect the difference between $\bar{\varphi}$ and φ in the right-hand member and postulate that

$$\Delta\,(\bar{\varphi} - \varphi) = 0 \ . \tag{6}$$

This is of course the slender-body approximation applied to the slot flow. There is additional support for its validity in that in transonic flow, and at low frequencies, all terms in the right-hand member of (1) are small. But this also points to the danger that the approximation (6) may not be very good near shock waves and high-frequency receding waves. At best the approximation can be verified a posteriori.

The differential equation (6) can be integrated immediately to give

$$\varphi = \bar{\varphi} + \phi - \bar{\phi} \ , \tag{7}$$

where $\phi(\underset{\sim}{r};x,t)$ and $\bar{\phi}(\underset{\sim}{r};x,t)$ are two-dimensional harmonic functions satisfying the same type of boundary condition as φ and $\bar{\varphi}$. More specifically, ϕ is taken to satisfy an inner condition (2) with the normal derivative prescribed as $f(P,t)$ on S_m (f being similar to, but in general different from F) and in addition to satisfy the condition (3) for the normal derivative at the outer boundary as well as the conditions (5) for the slot pressures (or a corresponding set for unsteady flow). In general this will determine ϕ uniquely in terms of f. Similarly, $\bar{\phi}$ is taken to satisfy the same inner boundary condition for the normal derivative as ϕ and a new homogeneous and local outer boundary condition chosen so as to make $\bar{\phi}$ uniquely determined and easy to calculate, rendering it at the same time closely equal to ϕ on S_m.

If the outer boundary condition for $\bar{\phi}$ has the required property of not containing f explicitly, then it might be eligible as the condition defining $\bar{\varphi}$. Let us assume this to be so and solve Eq. (1) for $\bar{\varphi}$, applying the inner boundary condition (2) together with the outer boundary condition thus taken over from $\bar{\phi}$. This can be done without specifying f. We then conclude from (7), assuming the basic approximation (6) to be true, that $\bar{\varphi}$ is closely equal to φ on S_m, as it should be.

The crucial question is now whether φ, as approximated by (7), satisfies the outer boundary conditions (3) and (5) to sufficient accuracy. To verify this, choose f so as to make $\bar{\phi}_n = \bar{\varphi}_n$ on S_w. The equality of $\bar{\phi}$ and $\bar{\varphi}$ on S_w (in virtue of the common boundary condition) is thereby extended, approximately, to a neighbourhood of S_w. Therefore, in consequence of (7), it might be assumed that in a similar neighbourhood (which is taken to include the slots) $\varphi \simeq \phi$, $\varphi_x \simeq \phi_x$, $\varphi_t \simeq \phi_t$, Grad $\varphi \simeq$ Grad ϕ, and also that the free boundaries S_p coincide. Then φ satisfies the boundary conditions (3) and (5), and the problem of computing φ on S_m, as influenced by the test section wall, has been reduced to the simpler problem of computing $\bar{\varphi}$.

Note that in this process it might be unnecessary to compute ϕ, f, or $\bar{\phi}$, since none of them is present in the boundary condition for $\bar{\varphi}$. However, if we want to determine conditions at the wall, for example wall pressures, then we shall need to know ϕ there.

5. Conformal Mapping and Analytic Continuation. Smoothing.

In order to arrive at the outer boundary condition for $\bar{\varphi}$ we must analyse ϕ and $\bar{\phi}$. They are both two-dimensional harmonic functions in regions with shapes independent of x. It is therefore natural to perform a conformal mapping of the annular region between S_w and S_m in each plane x = constant, mapping the boundaries onto concentric circles. In addition to other simplifications this will permit us to reformulate the inner boundary conditions for ϕ and $\bar{\phi}$ by analytic continuation to be imposed at the centre of the circles.

The mapping is scaled to leave the cross-sectional area of S_w invariant. Let (r,θ) be polar coordinates in the transformed plane. Hence S_w is mapped onto the unit circle.

We now postulate that in analysing $\bar{\phi}(r,\theta;x,t)$ it is sufficient to include only terms up to and including the order υ in a Fourier expansion with respect to θ. This is a decisive step: it specifies a 'filter' which permits us, by choice of υ, to approximate ϕ by $\bar{\phi}$ with controllable smoothness at the wall and precision at the model. Then $\bar{\phi}$ must have the form

$$\bar{\phi} = A_o \ln r + \bar{D}_o + \sum_{j=1}^{\upsilon} \Big[(A_j \cos j\theta + B_j \sin j\theta) r^{-j} + (\bar{D}_j \cos j\theta + \bar{E}_j \sin j\theta) r^{j} \Big] \ , \tag{8}$$

where the coefficients A_o, A_j, B_j, $\bar{D}_j$ and $\bar{E}_j$ are all functions of x and t.

The corresponding expression for $\phi(r,\theta;x,t)$, having the same singular structure at the origin, is

$$\phi = A_o \ln r + D_o + \sum_{j=1}^{\upsilon} \Big[(A_j \cos j\theta + B_j \sin j\theta) r^{-j} + (D_j \cos j\theta + E_j \sin j\theta) r^{j} \Big] + \delta \ , \tag{9}$$

where the remainder δ, containing the harmonic components required for describing details of the slot flow, is $O(r^{\upsilon+1})$ as $r \to 0$. In this formulation the requirement of common singular structure corresponds to the condition that the $\bar{\phi}$ and ϕ have the same normal velocity on S_m, while the requirement that the outer boundary condition for $\bar{\phi}$ shall make it closely equal to ϕ on S_m now takes the form

$$\bar{D}_o = D_o \ ; \quad \bar{D}_j = D_j \ , \qquad \bar{E}_j = E_j \quad (j = 1,2,\ldots,\upsilon) \ . \tag{10}$$

Once the outer boundary condition has been established we can either use it directly to solve the complicated transformed version of the transonic differential equation, or transform it back to the original geometry and there apply it to the simpler original equation. The choice is one of convenience in the numerical work. In the following we shall be concerned only with establishing the outer boundary condition in the circular geometry.

6. Asymptotic Approximation for Narrow Slots

The fact that in practice slots are usually narrow as compared to distances between slots will be the basis for the continued analysis. In this situation asymptotic expansion with respect to the slot width as a small parameter suggests itself as a useful method to be adopted. Obviously, each slot will need its own 'inner' expansion, scaled with the slot width. The 'outer' expansion will be concerned with the overall flow on the scale of the test section radius.

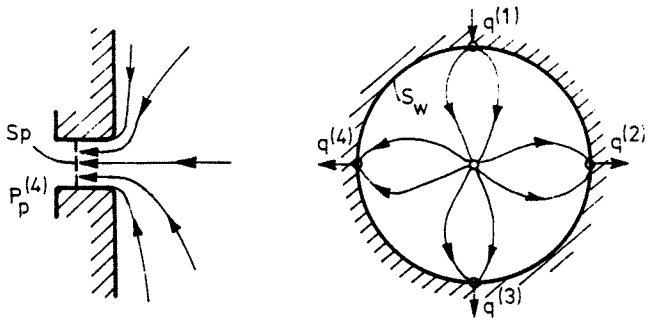

Fig. 3. Inner and outer flows.

In an inner expansion the slot will be located alone in an infinite plane wall (Fig. 3). In the outer expansion the test section wall will be solid with sinks or sources located at the points into which the slots have contracted. The total flux of each sink or source will of course be equal to twice the corresponding flux $q^{(i)}(i = 1,2,\ldots,N)$ through the slot (positive if into the plenum chamber; flux unit = U times test section radius). These fluxes are not known in advance but depend on the plenum pressures $p_p^{(i)}$ through the pressure conditions (5) at the boundaries S_{po} and S_p. They will therefore have to be obtained by matching the outer expansion to each of the inner expansions. For a survey of matching problems involving flow through narrow slots see Ref. 12.

Leaving the inner expansions for later, we shall first obtain an outer representation of ϕ, assuming the fluxes $q^{(i)}$ to be known. This will permit us to analyse $\bar{\phi}$ and, in fact, to make a first specification of the boundary condition for $\bar{\phi}$.

An elementary solution with a source at the origin and a sink of double strength on the unit circle at $\theta = \theta^{(i)}$ (Fig. 4) is given by $(1/2\pi)\ln r - (1/\pi)\ln r^{(i)}$, where $r^{(i)}(r,\theta)$ is the distance from the sink:

$$r^{(i)} = \sqrt{1-2r\cos(\theta-\theta^{(i)}) + r^2}\,. \qquad (11)$$

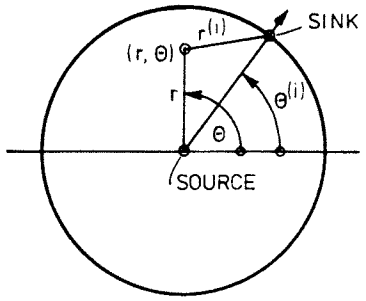

Fig. 4. A source at the origin, a sink of double strength on the unit circle.

It is easily shown that this solution has zero normal derivative on the unit circle (for $\theta \neq \theta^{(i)}$). We can therefore immediately write down the outer representation of ϕ :

$$\phi = \frac{1}{2\pi}\Big(\sum_{i=1}^{N} q^{(i)}\Big)\ln r - \frac{1}{\pi}\sum_{i=1}^{N} q^{(i)}\ln r^{(i)} + G(r,\theta). \qquad (12)$$

The undetermined function G is harmonic in the unit disk, except at the origin, and has zero normal derivative at the outer boundary. Comparison with (9) shows that $A_o = \Sigma\, q^{(i)}/2\pi$ and that

$$G = D_o + \sum_{j=1}^{U}(A_j\cos j\theta + B_j\sin j\theta)(r^{-j} + r^j). \qquad (13)$$

To obtain $\bar{\phi}$ we must expand the rest of ϕ. It is easy to show that

$$\ln r^{(i)} = -\sum_{j=1}^{U}\frac{1}{j}\cos[j(\theta-\theta^{(i)})]r^j + O(r^{U+1}), \qquad (14)$$

Hence

$$\bar{\phi} = \frac{1}{2\pi}(\Sigma q^{(i)})\cdot\ln r + D_o +$$

$$+ \frac{1}{\pi}\Sigma q^{(i)}\Big\{\sum_j \frac{1}{j}\cos[j(\theta-\theta^{(i)})]r^j\Big\} +$$

$$+ \sum_{j=1}^{U}(A_j\cos j\theta + B_j\sin j\theta)(r^{-j} + r^j) =$$

$$= \phi + \frac{1}{\pi}\sum_{i=1}^{N} q^{(i)}\Big\{\ln r^{(i)} + \sum_{j=1}^{U}\frac{1}{j}\cos[j(\theta-\theta^{(i)})]r^j\Big\}. \qquad (15)$$

This gives immediately an important part of the attempted outer boundary condition for $\bar{\phi}$:

$$r = 1: \quad \bar{\phi}_r = \frac{1}{\pi}\sum_{i=1}^{N} q^{(i)}\Big\{\frac{1}{2} + \sum_{j=1}^{U}\cos[j(\theta-\theta^{(i)})]\Big\}. \qquad (16)$$

This expression for the normal derivative of $\bar{\phi}$ at the outer boundary does not contain explicitly the coefficients A_j and B_j, which represent the shape of the model, and so it seems to be local as well as homogeneous in the previously defined sense. One might suspect that the unknown fluxes $q^{(i)}$, when resolved, will bring the

model back into the picture, but since they are to be obtained by matching at the slots we expect them, of course, to be locally determined in terms of $\bar{\phi}$.

In preparation for the matching we deduct from (15) the following inner representation of the outer representation of ϕ at the slot point k :

$$\phi = -\frac{q^{(k)}}{\pi} \ln r^{(k)} + \bar{\phi}(1,\theta^{(k)};x;t) + \sum_{i=1}^{N} q^{(i)} H^{(i,k)} + O(r^{(k)}) . \tag{17}$$

Here

$$H^{(i,k)} = -\frac{1}{\pi} \ln r^{(i,k)} - \frac{1}{\pi} \sum_{j=1}^{\upsilon} \frac{1}{j} \cos[j(\theta^{(k)} - \theta^{(i)})], \; i \neq k ,$$

$$H^{(k,k)} = -\frac{1}{\pi} \sum_{j=1}^{\upsilon} \frac{1}{j} , \qquad (i,k = 1,\ldots,N) , \tag{18}$$

with $r^{(i,k)}$ denoting the distance between the slot points i and k . The dominating part of the remainder corresponds to a tangential flow past the slot point.

7. Inner Representations and Matching

The inner flows might be analysed either in the transformed or the original cross-flow plane since the matching will involve only ϕ and the $q^{(i)}$, which are all invariant under the conformal mapping. We choose to work in the original plane as being clearly the simplest alternative.

As explained in general terms in Section 2, we shall work with a simplified slot flow model (Fig. 1) in which fast air from the test section enters the plenum chamber as a jet while, in reverse flow, the fast air in the slot returns to the test section without separation, letting in quiescent air behind it to form a longitudinal separation bubble at plenum pressure $p_p^{(k)}$. Since the boundary S_p between the two masses of air is not precisely defined in the model, we can use this freedom to simplify the computation of the inner representation. More specifically, we shall assume, at least in the steady case, that for any given family of similar slot cross-sections we can restrict ourselves to one basic cross-flow solution, taking the different positions of one of its material curves to represent possible free-boundary curves S_p. Then the slot flow model is essentially complete as soon as we prescribe the curve S_{po} at which the pressure condition is to be satisfied when there is a jet into the plenum chamber and at which the jet is to be taken to split when the flow reverses. Introducing Cartesian coordinates (z,y) (Fig. 5), we take as the parameter for any curve S_p its intersection y_p with the y-axis; y_{po}, the maximum value of y_p, corresponds to S_{po}.

Now let $a(x)$ be a measure of the width of the slot. The velocity level in the slot and its neighbourhood is given by $q^{(k)}/a$. With this should be compared the velocity set up by a streamwise variation of the slot width, as expressed by the normal velocity H in (3). As this is proportional to da/dx, it is evidently two orders of magnitude smaller in the limit

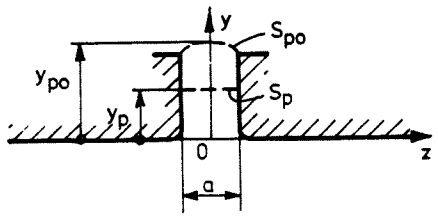

Fig. 5. Slot geometry.

$a \to 0$ and we can therefore safely neglect it when computing the cross flow. In addition to a sink-like flow into the slot, the geometry allows a flow essentially parallel to the wall. Its velocity is determined by the outer flow and is consequently $O(q^{(k)})$. We can neglect this flow component, too, when writing down the inner representation of ϕ to the lowest order; it should be included in the next order approximation, however.

We first solve the sink-flow problem with $a = 1$, $q^{(k)} = 1$ and with vanishing potential at $y = z = 0$. (How this can be done is demonstrated in Appendix 2 for the particular geometry of Fig. 5.) Let this normalized potential be $Q(z,y)$. Then our inner representation is

$$\phi = \phi^{(k)} + q^{(k)} \cdot Q(z/a, y/a) , \tag{19}$$

where $\phi^{(k)}(x,t)$ is the value of ϕ for slot k at $y = z = 0$ (if necessary extrapolated from S_p by Q) .

Far away into the test section Q has the representation

$$Q(z,y) = -\frac{1}{\pi} \ln r^{(k)} + R + O\left(\frac{1}{r^{(k)}}\right) ,$$

where

$$R = \lim_{r^{(k)} \to \infty} \left(Q + \frac{1}{\pi} \ln r^{(k)} \right) . \tag{20}$$

The corresponding representation of ϕ is

$$\phi = \phi^{(k)} - \frac{q^{(k)}}{\pi} \ln(r^{(k)}/a) + q^{(k)} R + O\left(\frac{a}{r^{(k)}}\right) ,$$

and this can be matched to the outer representation (17). Hence

$$\phi^{(k)} = \bar{\phi}(1,\theta^{(k)};x,t) + \sum_{i=1}^{N} q^{(i)} H^{(i,k)} - q^{(k)}\left(\frac{1}{\pi} \ln a + R\right) . \tag{21}$$

This important result permits us to relate $\bar{\phi}$ locally to the plenum pressures.

8. The Plenum Pressure Condition in Steady Flow

So far the analysis applies in its main features to unsteady as well as steady flow. We now restrict ourselves to the steady case (to return later for a brief discussion of the un-

steady case). We can then apply the pressure condition (5), which gives at $z = 0$, $y = y_p$ or y_{po}

$$\phi_x + \frac{1}{2}\left(\frac{q^{(k)}}{a} v_p\right)^2 = -\delta^{(k)} \quad , \tag{22}$$

where $v_p(y_p/a)$ is the value of the y-derivative of the normalized potential Q at $z = 0$ on S_p. It is sufficient to satisfy the condition at $z = 0$ if the variation of flow velocity on the boundary curve is small, as we shall assume in concordance with our simplified description of S_p. In order to keep track of $y_p(x)$ when it is smaller than y_{po} one has to solve the differential equation

$$\frac{dy_p}{dx} = \frac{q^{(k)}}{a} v_p(y_p/a) \quad , \tag{23}$$

marching downstream from $x = x_o$, where $y_p = 0$, and taking a new initial value y_{po} each time the jet splits on flow reversal.

Inserting ϕ from (19) into (22), with $\phi^{(k)}$ from (21), we obtain the pressure condition in the form

$$\frac{d}{dx}\left\{\bar{\phi}(1,\theta^{(k)};x) + \sum_{i=1}^{N} q^{(i)} H^{(i,k)} + \right.$$

$$\left. + q^{(k)}\left[Q(0\ y_p/a) - R - \frac{1}{\pi} \ln a\right]\right\} +$$

$$+ \frac{1}{2}\left(q^{(k)} v_p/a\right)^2 = -\delta^{(k)} \quad (k = 1,\ldots,N) \quad . \tag{24}$$

If all the fluxes $q^{(i)}(x)$ are known this is an ordinary differential equation for $\bar{\phi}(1,\theta^{(k)};x)$ which can be integrated together with (23), starting with a known value for $\bar{\phi}$ at the beginning of the slot.

9. On Outer Boundary Conditions for Transonic Flows

At this stage, before we attempt to construct an outer boundary condition from the raw material gathered in the preceding sections, it might be useful to consider what sort of a boundary condition we should like to have.

We are now concerned with steady flows only, so the differential equation with which to use the boundary condition is

$$\Delta\bar{\varphi} = [M^2 - 1 + M^2(\gamma+1)\bar{\varphi}_x]\bar{\varphi}_{xx} \quad . \tag{25}$$

Typically, with those unbounded transonic flows for which the small-perturbation analysis is valid, the right-hand member is small compared to the cross-flow derivatives constituting the left-hand member. We expect this to be true also in the present case, at least to the extent that we have been successful in designing a slotted test section with small interference. This means of course that the cross flow in any plane x = constant is approximately volume conserving so that as much volume flux as entering at the inner boundary, there determined by the shape of the model, must leave through the outer boundary at about the same cross section. This constitutes a strong restriction on $\bar{\varphi}_n$ at the outer boundary in terms of $\bar{\varphi}_n$ at the inner boundary, suggesting that we might run into difficulties if we try to prescribe the normal derivative at the outer boundary.

These considerations come sharply into focus in the case of axisymmetric flow in the slender-body approximation, that is with the right-hand member of (25) neglected. Then the perturbation potential $\bar{\varphi}(x,r)$ takes the form

$$r\bar{\varphi}_r = s'(x), \quad \bar{\varphi} = s'(x) \cdot \ln r + \bar{\varphi}(x,1) \quad ,$$

where $s(x)$ is essentially the cross-sectional area of the body. In this case the radial velocity is everywhere exactly determined by the inner boundary condition, at the body, and only the potential itself can be prescribed at an outer boundary (at $r = 1$, say). Therefore we obtain a reasonable slender-body solution if the outer boundary is a jet boundary at prescribed pressure, or a ventilated wall which responds to the radial velocity $s'(x)$ with a well-defined pressure distribution. On the other hand, with a solid wall, at which zero normal derivative must be prescribed, there is no solution at all. Then the right-hand member must be retained in (25), accounting for the raised blockage interference level typical of choking.

We shall therefore attempt to obtain our outer boundary condition in the form

$$\text{on } S_w: \quad \bar{\varphi} = \mathcal{F}[\bar{\varphi}_n] \quad , \tag{26}$$

where $\mathcal{F}[\ ]$ is a regular functional over S_w (it becomes singular in the limit of a solid wall, of course). This choice carries with it the suggestion that in solving (25) by an iterative numerical method one should march back and forth between the model and the outer boundary, arriving each time at the outer boundary with an improved normal velocity to give, by (26), an improved pressure distribution to be carried back to the model. It is reassuring to be able to note that employing such a scheme speeds up convergence, in particular in subsonic regions.[13] Our philosophy also suggests that the finite-difference approximation for the left-hand member of (25) should be a conservative one.

The choice of (26) should not, however, preclude interest in the inverse functional, $\mathcal{F}^{-1}$, giving $\bar{\varphi}_n$ in terms of $\bar{\varphi}$. Actually, if we are to adopt the idea of a 'self-correcting' test section, presently being pursued in several laboratories, then a viable scheme might be to measure the wall pressure distribution along slats, essentially φ, and hence compute the normal velocity $\bar{\varphi}_n$ rather than trying to measure it. For this $\mathcal{F}^{-1}$ would be needed (together with a procedure for obtaining $\bar{\varphi}$ from φ; see Section 12). One would next have to compute the unbounded flow outside S_w, using $\bar{\varphi}_n$ in an inner boundary condition and obtaining an estimate of what $\bar{\varphi}$ should be on S_w in order to be free of interference. Using again the same $\bar{\varphi}_n$, one would then adjust the test parameters so as to make $\bar{\varphi}$, computed by (26) with the adjusted $\mathcal{F}$, equal to $\bar{\varphi}$ obtained from the outer flow. Repeating this cycle as long as the re-

quired wall adjustments can be realized, employing alternately $\mathcal{F}^{-1}$ and $\mathcal{F}$, one should end up with a slotted wall of minimum interference. Running the cycle backwards, adjusting $\bar{\varphi}_n$ for equality rather than $\bar{\varphi}$, would seem to be inviting difficulties.

10. Constructing the Outer Boundary Condition

According to the prescription of Section 4 for the boundary condition on S_w, $\bar{\varphi}$ is to be related to $\bar{\varphi}_n$ in the same way as $\bar{\phi}$ is related to $\bar{\phi}_n$. To the extent that we have established this relationship it is contained in Equations (16), (23) and (24).

We take (16) as a starting point since it contains the normal derivative, the argument function of $\mathcal{F}$. Substituting $\bar{\varphi}(x,r,\theta)$ for $\bar{\phi}(r,\theta;x)$ and specializing θ to the slot positions, we obtain

$$\sum_{i=1}^{N} \left\{ \frac{1}{2} + \sum_{j=1}^{\upsilon} \cos[j(\theta^{(k)} - \theta^{(i)})] \right\} q^{(i)} = \pi \cdot \bar{\varphi}_r(x,1,\theta^{(k)}) \quad (k = 1,2,\ldots,N) \; . \tag{27}$$

This a linear system which determines, for each x, the slot fluxes in terms of $\bar{\varphi}_r$. The coefficient matrix is independent of x and can be inverted numerically and stored as soon as the slot locations have been decided. Thus it is very simple to calculate the slot fluxes from $\bar{\varphi}_r$.

Next we integrate the equations (23) to determine the flow penetration depth in the slots. This is straightforward, taking one slot at a time. Now the slot geometry is involved, however, so the integration must be repeated each time we make a wall adjustment.

From (24), finally, we obtain the value of the potential at the slot positions,

$$\bar{\varphi}(x,1,\theta^{(k)}) = \varphi_o - [Q(0,y_p/a) - R - \frac{1}{\pi} \ln a] q^{(k)} - \sum_{i=1}^{N} H^{(i,k)} q^{(i)} - \int_{x_o}^{x} \left[\frac{1}{2} (q^{(k)} v_p / a)^2 + \delta^{(k)} \right] dx \quad (k = 1,\ldots,N), \tag{28}$$

satisfying at $x = x_o$ the upstream condition for $\bar{\varphi}$ assumed in Section 3. The right-hand member is now completely known. It would remain valid if we were to allow the plenum pressures to vary with x.

It is primarily Equation (28) we must analyse when we want to adjust slot flow parameters so as to produce the wall pressure distribution corresponding to interference-free flow. There will always be interference around the entrance section at $x = x_o$. The test parameters, including the direction of the unbounded flow we are trying to simulate, should be selected in such a way as to make this interference small and local. Also, note the singular behaviour of $\bar{\varphi}$ at x_o, where not only a vanishes but also $q^{(k)}$ (since Grad $\bar{\varphi} = 0$ over the whole plane $x = x_o$). One cannot expect

$$\bar{\varphi}_x(x_o,1,\theta^{(k)}) = -\left[\frac{1}{2} \left(v_{p\,\lim_{x \to x_o}} \frac{q^{(k)}}{a} \right)^2 + \delta^{(k)} \right]$$

to be well-determined since $\lim(q^{(k)}/a)$ will never be known with any precision. This gives us, perhaps, the opportunity to specify $\lim(q^{(k)}/a)$, which is also needed in Eq. (23), in such a way that $\bar{\varphi}_x$ takes the value corresponding to the chosen entrance Mach number M_o, thus avoiding a spurious velocity jump at $x = x_o$. In practice the achievement of a smooth entrance flow might require a proper choice of plenum pressures.

In order to complete the construction of the functional $\mathcal{F}$ we have only to define $\bar{\varphi}$ between slots. In accordance with our method of analysis this is done, in each plane $x = \text{constant}$, by trigonometric interpolation of order υ. Obviously υ must be chosen so as to make $2\upsilon + 1$ equal to N at most ; usually it will be smaller. This means that usually we cannot satisfy the conditions (28) precisely. A least-squares fit could then be used, which again calls for storing a pre-computed constant matrix. The deviations, of course, correspond to higher order components to be filtered out. Since both (23) and (28) are non-linear with respect to $q^{(i)}$ such components will arise even if not present in the $\bar{\varphi}_r$ used in (27).

The inverse functional is not so easily constructed, due to the non-linearity of the equations from which are determined the fluxes $q^{(i)}$ corresponding to a given potential on S_w. An iterative scheme must be set up. Once the fluxes are known, the normal derivative is immediately obtained from (27) at the slot positions. The construction is again completed by trigonometric interpolation.

11. Symmetric Flow

As a simple application consider the case of an axisymmetric body along the axis of a circular test section with N uniformly distributed identical slots ($N > 1$). From symmetry, the flow is periodic with respect to θ with period $2\pi/N$. The potential φ will therefore be independent of θ to order $N-1$ in a trigonometric expansion. Since $N-1$ is larger than $(N-1)/2$, the upper bound for υ, we conclude that $\bar{\varphi}$ is independent of θ. Actually, since the flux through each slot is given by

$$q = d\, \bar{\varphi}_r(x,1), \quad d = \frac{2\pi}{N} \; (= \text{arc length between slots}) \tag{29}$$

and is independent of υ, we will get the same $\bar{\varphi}(x,r)$ for all permitted values of υ.

Equation (29) takes the place of (27). It remains to consider (23) and (28). Noting that in the present case

$$\sum_{i=1}^{N} H^{(i,k)} = -\frac{1}{\pi} \ln N \; ,$$

we obtain

$$\frac{dy_p}{dx} = v_p \frac{d}{a} \bar{\varphi}_r(x,1) \; , \tag{30}$$

and

$$\bar{\varphi}(x,1) = \varphi_o - K\bar{\varphi}_r(x,1) - \int_{x_o}^{x}\left[\frac{1}{2}\left(v_p\,\frac{d}{a}\,\bar{\varphi}_r\right)^2 + \delta\right]dx, \quad (31)$$

with

$$K = d\left[\frac{1}{\pi}\,\ell n\,\frac{2d}{\pi a} - \frac{1}{\pi}\,\ell n\,4 - R + Q(0, y_p/a)\right] . \quad (32)$$

Equation (31) agrees with the classical formula, augmented by a quadratic cross-flow term in the manner of W.W. Wood[14]. It is shown in Appendix 2 that Equation (32) is a second order approximation for small a/d to the classical as well as the generalized[4] K.

It may seem remarkable that $\bar{\varphi}$ is independent of θ. It does not mean, however, that the wall interference is totally independent of the number of slots, not even for a fixed $\bar{\varphi}$. In adding slots we suppress successively higher harmonics which were neglected in $\bar{\varphi}$ (but present in φ) when the slots were fewer.

The outer boundary condition $\bar{\varphi} = \mathcal{F}[\bar{\varphi}_r]$ as constituted by Equations (30), (31) and (32) has been tested quite extensively[4] with the numerical method of Ref. 13. No difficulties were found except where the slot width was very small, smaller than normally used, in which case the convergence became slow. This is of course not surprising since $\mathcal{F}$ is singular in the limit of a solid wall.

12. Analysis of Wall Pressures

For a further application, assume that we want to determine $\bar{\varphi}$ on S_w by measuring the pressure distribution along slats, at constant $\theta = \theta_w \neq \theta^{(i)}$ say. We first integrate (4) along the slat to get φ (the quadratic cross-flow term can be neglected in this case). Then from Equations (7) and (15) we have

$$\bar{\varphi} = \varphi + \bar{\phi} - \phi$$

$$= \varphi + \frac{1}{\pi}\sum_{i=1}^{N} q^{(i)}\left\{\ell n\, r_w^{(i)} + \sum_{j=1}^{\upsilon}\frac{1}{j}\cos\left[j\left(\theta_w - \theta^{(i)}\right)\right]\right\} \quad (33)$$

where $r_w^{(i)}$ is the cross-flow distance from a pressure tap to the slot point i. In the case of symmetric flow with θ_w half way between slots this reduces to the result obtained in Ref. 4.

The application of (33) is straightforward if we know the fluxes, but we don't in the interesting case when we want to determine $q^{(i)}$ and $\bar{\varphi}_r$ by applying $\mathcal{F}^{-1}$ to $\bar{\varphi}$. However, $\bar{\varphi} - \phi$ has the character of a small correction, so there is little doubt that an iterative scheme, using successively improved estimates for $q^{(i)}$, will converge rapidly. This is not really very much of a complication. $\mathcal{F}^{-1}$ has to be computed iteratively anyway.

13. Unsteady Flows

In the first seven sections the analysis applies in its main features also to unsteady flows. In the pressure condition (5), however, we must add φ_t/U to φ_x, recognizing at the same time that the free surface S_p might move and that the plenum pressures $\delta^{(i)}$ are no longer known in advance since pressure waves may propagate into the plenum chamber. The simplified picture of the slot flow introduced in Section 7 should be extended to include a potential which describes the cross flow due to the motion of S_p, in addition to the potential Q which describes the cross flow due to the obliqueness of the flow. (This approach means, of course, that we are assuming the slot width to be small compared to typical wave lengths of the unsteady flow.) The additional cross flow is somewhat different in that it involves the quiescent air of the plenum chamber as well as the fast air in the slot. This will also add a new contribution to the right-hand member of Eq. (23) for S_p, the left-hand member of which, of course, now becomes $[\partial/\partial x + (1/U)\partial/\partial t]y_p$. All these effects combine to make the pressure condition corresponding to (24) rather complicated in its final form.

In order to account for fluctuations in $\delta^{(i)}$, we must analyse the wave propagation in the plenum chamber, a forbidding task. The simplest case arises if the plenum chamber is so large that only waves propagating from the slots into the plenum chamber contribute to the pressure fluctuation on $S_{po} + S_p$. These waves correspond to the additional, non-steady part of the slot flow and so can be analysed, assuming a known steady pressure deeper inside the plenum chamber. In the next more complicated case one would have to account for varying plenum pressure in the manner of the classical Helmholtz resonance analysis. It seems that in these two cases there is a reasonable chance to be able to complete the analysis and construct a homogeneous boundary condition for the test section flow. It will perhaps be necessary to linearize the problem, assuming the unsteadiness to be a small perturbation of a steady flow.

14. Wall Interference Corrections. Test Section Calibration.

Suppose we have succeeded in adjusting the test parameters so as to make the interference negligible at the model. Then three wall corrections of classical type are immediately available from this process: a Mach number correction $(= M - M_o)$, an angle-of-attack correction (= the angle of attack of the test section with respect to the direction of the unbounded flow simulated), and an angle-of-yaw correction (= the corresponding angle of yaw of the test section).

The other classical corrections, those for induced buoyancy and flow curvature, are rightly absent. As soon as they are needed there is a distortion of the pressure distribution over the model that cannot be tolerated. In contrast, the former corrections are not associated with any such distortion and should be permitted to be large if it helps in reducing the interference. This is "the principle of minimizing interference rather than corrections"[15], implying the concept of a "correctable-interference transonic wind tunnel"[16].

There might be other errors present in the test section flow, errors which are not accounted for when computing the wall interference. Disturbances from the entrance section upstream of

the slots, axial gradients set up by the wall boundary layers or by improper alignment of the walls, or upstream influence from the sting arrangement are examples. The main tool for handling such errors is "calibration", running the test section empty with the walls and plenum pressures set for uniform flow. Such errors should be eliminated by proper adjustment of the test section, not by introducing corrections to the test data. The practice of using the Mach number of the empty test section, calibrated against the plenum pressure, as a free-stream reference Mach number for model tests does not seem to make sense in the context of the present theory.

15. Concluding Remarks

The present inviscid theory of wall interference in slotted test sections generalizes to three-dimensions the theory for two-dimensional tests developed on a classical basis[5,14] in Ref. 4. In analysing the local flow at each slot separately, the structure of the theory is such as to facilitate later inclusion of corrections to account for viscous effects inside the slots and the plenum chamber. A first attempt in this direction has already been made[4] and as more extensive comparisons with experiment are completed it might become possible to extend and delineate the area where the inviscid theory, with or without corrections, might be used with confidence. The interaction of shock waves with the slot flow must be studied, in particular.

Meanwhile the inviscid theory can be used for running numerical experiments. These will show how accurately one must describe the action of the slotted wall in different types of application, and what wall adjustment facilities one must provide in order to eliminate the wall interference. They will also help developing strategies for efficient use of adjustable slotted walls in future wind tunnels.

References

1. Wright, R.H., The effectiveness of the transonic wind-tunnel as a device for minimizing tunnel-boundary interference for model tests at transonic speeds. AGARD Rep. 294 (1959).

2. Goethert, B.H., Transonic wind tunnel testing. Edited by W.C. Nelson. AGARDograph 49. Pergamon Press 1961.

3. Berndt, S.B., Theory of wall interference in transonic windtunnels. Symposium Transsonicum (1962), edited by K. Oswatitsch, pp. 288-309. Springer-Verlag 1964.

4. Berndt, S.B. and Sörensén, H., Flow properties of slotted walls for transonic test sections. AGARD Conf. Proc. No. 174, Paper No. 17 (1975).

5. Guderley, G., Simplifications of the boundary conditions at a wind-tunnel wall with longitudinal slots. Wright Air Development Center Tech. Rep. 53-150 (1953).

6. Baldwin, Jr., B.S., Turner, J.B. and Knechtel, E.D., Wall interference in wind tunnels with slotted and porous boundaries at subsonic speeds. NACA TN 3176 (1954).

7. Davis, D.D. and Moore, D., Analytical studies of blockage- and lift-interference corrections for slotted tunnels obtained by the substitution of an equivalent homogeneous boundary for the discrete slots. NACA RM-L53E07b (1953).

8. Maeder, P.F., Theoretical investigation of subsonic wall interference in rectangular slotted test sections. Brown Un., Div. of Engineering, Tech. Rep. WT-11 (1953).

9. Woods, L.C., The theory of subsonic plane flow. Cambridge 1961.

10. Barnwell, R.W., Improvements in the slotted-wall boundary condition. Proc. AIAA 9th Aerodynamic Testing Conf., p. 21 (1976).

11. Garner, H.C. et al., The theory of interference effects on dynamic measurements in slotted-wall tunnels at subsonic speeds and comparison with experiment. A.R.C. R. & M. 3500 (1966).

12. Tuck, E.O., Matching problems involving flow through small holes. Adv. Appl. Mech. 15, 90 (1975).

13. Sedin, Y.C.-J., Axisymmetric sonic flow computed by a numerical method applied to slender bodies. AIAA J. 13, 504 (1975).

14. Wood, W.W., Tunnel interference from slotted walls. Qu. J. Mech. Appl. Math. 17, 126 (1964).

15. Berndt, S.B., On the influence of wall boundary layers in closed transonic test sections. FFA Rep. 71 (1957).

16. Kemp, W.B., Jr., Toward the correctable-interference transonic wind tunnel. Proc. AIAA 9th Aerodynamic Testing Conf., p. 31 (1976).

Appendix 1 — Symbols

$a(x)$	Slot width; Fig. 5
d	Arc length between slots; Eq. (29)
Grad, $\underline{\Delta}$	Differential operators in plane x = constant
$\mathcal{F}$, $\mathcal{F}^{-1}$	Functionals on S_w ; Eq. (26)
$H^{(i,k)}$	Eq. (18)
$K(x)$	Coefficient in slotted-wall boundary condition; Eqs. (32), (A-8) and (A-12)
M	Mach number of reference flow
M_o	Entrance Mach number; Fig. 2
N	Number of slots
p	Pressure
$p_p^{(i)}$	Pressure in plenum chamber i
p_∞	Pressure of flow at Mach number M

$Q(z,y)$	Normalized slot flow potential; Eq. (19)
$q^{(i)}(x,t)$	Flux through slot i ; Eq. (12)
R	Eq. (20)
$\underset{\sim}{r}$	Radius vector in cross-flow plane
r, θ	Polar coordinates in cross-flow plane
$r^{(i)}$	Distance from slot point i ; Fig. 4, Eq. (11)
$r^{(i,k)}$	Distance between slot points i and k; Eq. (18)
S_m	Cylindrical surface enclosing the model and its wake; Fig. 2
S_p	Free surface between fast air and quiescent plenum air; Fig. 1
S_{po}	Surface at plenum pressure across jet on plenum side of slot; Fig. 1
S_w	Outer boundary of test section; Fig. 2
t	Time
U	Flow velocity at Mach number M
$v_p(y_p)$	$= \partial Q/\partial y$ at $y = y_p$, $z = 0$; Eq. (23)
x	Distance along tunnel axis; Fig. 2
x_o	Location of entrance section; Fig. 2
y,z	Cartesian coordinates at slot; Fig. 5
y_p	Coordinate of S_p on slot centre line; Fig. 5
y_{po}	Coordinate of S_{po} on slot centre line; Fig. 5
γ	Ratio of specific heats
$\delta^{(i)}$	Non dimensional plenum pressure difference; Eq. (5)
$\varphi, \bar{\varphi}$	Perturbation velocity potentials; Eqs. (1) and (6)
$\phi, \bar{\phi}$	Harmonic functions in cross-flow plane; Eq. (7)
υ	Highest order considered in harmonic analysis of interference; Eq. (8)
ϱ_∞	Density of flow at Mach number M

Appendix 2

Simplified Analysis of Slot Flow

As a basis for analysing the slot flow for the geometry of Fig. 5, consider the symmetrical flow of unit flux from a half plane into a slot of unit width and unlimited depth (see sketch).

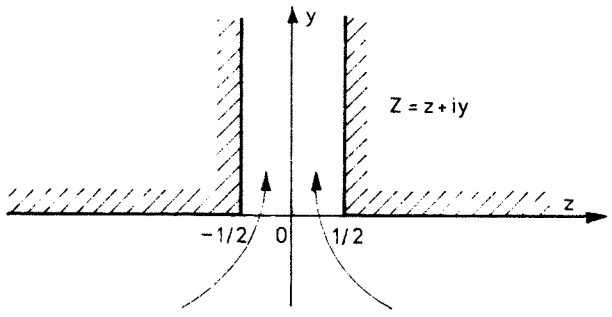

We shall determine the velocity potential $Q(y,z)$, normalized to vanish at the origin.

This is accomplished by mapping the flow region conformally onto a half plane ($-\pi \le \vartheta \le 0$ in sketch), transforming the slot extremity

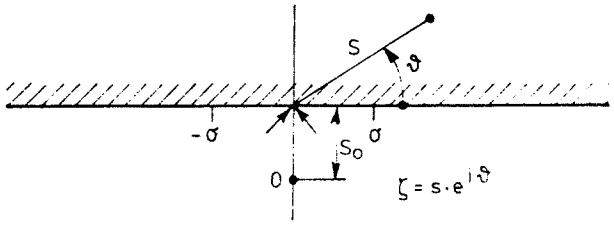

($Z = i\infty$) into the origin and leaving the far field undisturbed. The required complex transformation is

$$Z = z + iy$$

$$= e^{i\vartheta}\sqrt{s^2 - \sigma^2 e^{-2i\vartheta}} - i\sigma \ln \frac{\sqrt{s^2 - \sigma^2 e^{-2i\vartheta}} + i\sigma e^{-i\vartheta}}{s} ,$$

$$\sigma = \frac{1}{\pi} , \qquad \text{(A-1)}$$

where (s,ϑ) are polar coordinates in the transformed plane ζ. The exterior wall and the slot walls are mapped onto the real axis with the corner points at $\pm\sigma = \pm 1/\pi$. The origin goes into a point on the negative imaginary axis, at distance s_o from the origin, say. The flow is that of a sink at the origin, hence

$$Q = -\frac{1}{\pi} \ln \frac{s}{s_o} . \qquad \text{(A-2)}$$

This gives, according to Eq. (20), $R = (1/\pi) \ln s_o$.

As the material curve to represent, in its different positions, possible free-boundary curves S_m, we choose one which far into the slot is a straight line across the slot. In the transformed plane the curve, when close to the origin, is a circle. In order to determine its development we can integrate along streamlines (rays) in the transformed plane. Points on the same curve must have the same value of the parameter

$$t(s,\vartheta) = \int_{\varepsilon}^{s} \left|\frac{dZ}{d\zeta}\right|^2 s \, ds , \qquad \text{(A-3)}$$

where ε is a small positive number. After the curves have been determined in the ζ-plane they have to be transformed back into the Z-plane. This has not been carried out yet.

For our immediate purpose it is sufficient to consider the intersection y_p of S_m with the axis of symmetry. This point is mapped on the negative imaginary axis, at the distance s_p from the origin, say. The value of s_p is obtained from the equation

$$\sqrt{s_p^2 + \sigma^2} + \sigma \ln \frac{\sqrt{s_p^2 + \sigma^2} - \sigma}{s_p} = -y_p , \qquad \text{(A-4)}$$

which gives, in particular, $s_p = s_o = 0.2110$ for $y_p = 0$. Once $s_p(y_p)$ is known, it is straightforward to compute Q and v_p :

$$Q(0,y_p)-R=-\frac{1}{\pi}\,\ln s_p\,,\quad v_p=-\frac{1}{\pi}\,\frac{d\,\ln s_p}{d\,y_p}\,. \qquad (A-5)$$

If y_p is well inside the slot we can take s_p/σ to be small. Expanding the square root in (A-4), the following second order approximation is obtained:

$$-\ln s_p = 1-\ln\frac{2}{\pi}+\pi y_p+e^{-2(\pi y_p+1)}\,. \qquad (A-6)$$

Hence

$$Q(0,y_p)-R=\frac{1}{\pi}\left(1-\ln\frac{2}{\pi}\right)+y_p+\frac{1}{\pi}\,e^{-2(\pi y_p+1)}\,,$$

$$v_p(y_p)=1-2e^{-2(\pi y_p+1)}\,. \qquad (A-7)$$

Inserting into Eq. (32), we obtain

$$K=d\left[\frac{1}{\pi}\ln\frac{2d}{\pi a}+\frac{1}{\pi}\left(1-\ln\frac{8}{\pi}\right)+y_p/a+\frac{1}{\pi}\,e^{-2(\pi y_p/a+1)}\right], \qquad (A-8)$$

in complete agreement (to second order in a/d) with the result of Ref. 4, at least for $y_p/a>0.1$.

This result is valid if S_p is inside the slot. If the flow is leaving the slot as a jet into the plenum chamber the analysis in Ref. 4 shows that Eq. (A-8) is still valid if y_p/a is changed into $\ell/a+0.22$, where ℓ is the depth of the slot. In the present terminology this means simply that we shall take

$$\frac{y_{po}}{a}=\frac{\ell}{a}+0.22\,. \qquad (A-9)$$

When there is a 'bubble', for $y_p<0$, Eq. (A-4) can again be solved approximately. The result, for $s_p \gg \sigma$, is

$$s_p=-y_p\left(1+\frac{5}{8\pi^2}\,\frac{1}{y_p^2}\right), \qquad (A-10)$$

hence

$$Q(0,y_p)-R=\frac{1}{\pi}\ln y_p-\frac{5}{8\pi^3}\,\frac{1}{y_p^2}\,,$$

$$v_p=\frac{1}{\pi}\,\frac{1}{y_p}\left(1-\frac{5}{4\pi^2}\,\frac{1}{y_p^2}\right). \qquad (A-11)$$

This is consistent with S_p becoming approximately a semicircle with centre at the origin as soon as $|y_p|>a$. The corresponding result for K is

$$K=d\left[\frac{1}{\pi}\ln\frac{d}{2\pi|y_p|}-\frac{5}{8\pi^3}\,\frac{1}{(y_p/a)^2}\right]. \qquad (A-12)$$

Finally, it might be noted that the preceding analysis, with very minor modifications, applies also to a slot located in a right-angled corner. One has only to make the axis of symmetry into a wall and everything else follows.
